Scilight

Intelligence & Control
https://www.sciltp.com/journals/ic

Article

Observer-Based Finite-Horizon H_∞ Consensus Control of Multi-Agent Systems under Multi-Round-Robin Scheduling

Jiaxin Chen, Yezheng Wang * and Fan Wang

College of Automation, Nanjing University of Information Science and Technology, Nanjing 211800, China
* Correspondence: wangyz_sdust@163.com

How To Cite: Chen, J.; Wang, Y.; Wang, F. Observer-Based Finite-Horizon H_∞ Consensus Control of Multi-Agent Systems under Multi-Round-Robin Scheduling. *Intelligence & Control* **2026**, *2*(1), 3. https://doi.org/10.53941/ic.2026.100003

Received: 4 December 2025
Revised: 14 March 2026
Accepted: 23 March 2026
Published: 27 March 2026

Abstract: This paper investigates the finite-horizon H_∞ consensus problem for time-varying discrete-time multi-agent systems governed by a multi-Round-Robin scheduling protocol. Within a networked communication environment, the multi-Round-Robin protocol is employed to facilitate flexible and scheduled data exchanges among agents. To enhance the system's robustness against external disturbances, an observer-based cooperative control strategy is developed, utilizing the estimated states from neighboring agents. The primary objective is to design a distributed cooperative controller for each agent to ensure the prescribed H_∞ consensus performance over a finite time interval. Sufficient conditions for achieving the desired consensus behavior are derived, and both controller and observer parameters are determined by solving two coupled backward recursive Riccati difference equations. Finally, a numerical example demonstrates the effectiveness of the proposed approach and highlights the superiority of the multi-Round-Robin protocol over the conventional Round-Robin protocol.

Keywords: multi-agent systems; observer-based strategy; finite-horizon; H_∞ consensus; backward recursive Riccati difference equations; Round-Robin protocols

1. Introduction

Since the emergence in the 1970s, multi-agent systems (MASs) have undergone rapid development in both theoretical foundations and practical applications. The progress is largely attributed to MASs' inherent distributed computing capabilities, which make it able to solve problems that are intractable for single-agent approaches. As a result, MASs have attracted substantial research interest over the years. Recent decades, in particular, have witnessed significant advances and successful deployments of MASs across a variety of fields, such as sensor networks [1–3], microgrid power systems [4–6], unmanned aerial vehicles [7–9], and intelligent transportation [10–12]. It is worth noting that in real-world applications, MASs are often time-varying and inevitably subjected to various external disturbances and uncertainties. The widespread presence of such disruptions highlights the urgent need for robust consensus and control methodologies suitable for time-varying MASs [13,14].

As a fundamental issue in cooperative control of MASs, the consensus problem represents a central research direction in this field. The core objective of consensus control is to design distributed strategies that enable large-scale systems composed of multiple agents to achieve global state consensus or behavioral coordination using only local neighborhood interactions. With advances in algebraic topology and control theory, a multidimensional research framework has been established, covering continuous-time and discrete-time settings, as well as deterministic and stochastic scenarios. A variety of advanced methodologies have been developed to tackle consensus challenges, such as adaptive distributed dynamic event-triggered observers for directed graph topologies [15], distributed intermediate estimators for fault-tolerant control [16], and improved dynamic adaptive event-triggering mechanisms for nonlinear MASs [17]. In response to practical engineering needs, several variants of consensus have also been extensively investigated, including quasi-consensus [18,19], bipartite consensus [20,21], and scaled consensus [22,23].

With the increasing scale of MASs, network data transmission has become a critical bottleneck limiting further improvement of system performance [24]. In typical application domains such as industrial automation, intelligent transportation, and distributed robotics, the expansion of system size requires communication networks to handle exponentially growing volumes of information exchange [25]. Traditional analytical models for networked systems often rely on the assumption of infinite bandwidth in communication links. Although such an idealized assumption simplifies theoretical analysis, it significantly diverges from real-world network environments. In practice, communication constraints due to limited bandwidth lead to several issues, including packet loss, out-of-order data delivery, and transmission delays. To address the network-induced challenges, the design of effective communication protocols has emerged as a key technical pathway for enhancing the performance of networked systems.

Various communication protocols have been developed and widely adopted in networked control systems to address these challenges. Common communication protocols primarily include stochastic communication protocols [26–28], which employ probabilistic mechanisms to manage network access and are particularly suitable for systems with uncertain communication conditions; Round-Robin protocols [29–31], which provide deterministic and fair scheduling by allocating transmission rights in a fixed cyclic order; and weighted try-once-discard protocols [32–34], which prioritize data freshness by discarding outdated information based on weighted importance metrics. The Round-Robin protocol is a classical scheduling mechanism that ensures fair and deterministic communication access in networked systems by allocating transmission rights to each node in a fixed cyclic order. This approach guarantees collision-free data exchange and predictable channel utilization for industrial control systems. In practical networked systems, communication bandwidth is typically limited, although a fixed number of concurrent transmissions are usually permitted. The traditional Round-Robin protocol is relatively conservative in communication scheduling. In large-scale multi-agent systems, where each agent may have many neighboring nodes, the polling period for each communication link becomes long, resulting in inefficient information exchange. In contrast, the multi-Round-Robin protocol extends the conventional framework by introducing multiple overlapping Round-Robin sequences with differentiated scheduling periods or priority levels. The enhanced architecture allows for more flexible bandwidth allocation, supports heterogeneous node priorities, and enables adaptive scheduling in dynamic environments, which can significantly accelerate the convergence speed of consensus algorithms. Moreover, by adjusting the number of concurrent transmissions, the protocol provides a flexible mechanism to balance communication overhead and control performance. Despite existing research on control of MASs with Round-Robin protocols, e.g., [35, 36], a critical gap remains in the study of the multi-Round-Robin protocol, where [37] represents one of the few initial efforts.

Given the dynamic and complex nature of real-world environments, agents are often affected by exogenous disturbances and measurement uncertainties, making robustness a fundamental requirement in consensus control design. As an effective robust control framework, H_∞ control has attracted sustained attention because it can attenuate the influence of worst-case disturbances while providing guaranteed performance levels for closed-loop systems. Although considerable progress has been achieved in H_∞ control of MASs, e.g., [13, 38, 39], the development of finite-horizon observer-based H_∞ consensus schemes for time-varying MASs under practical communication scheduling constraints is still insufficient. Therefore, it is both theoretically meaningful and practically important to investigate the observer-based finite-horizon H_∞ consensus control problem in such networked environments.

Based on the preceding analysis, this paper presents a comprehensive study on the observer-based finite-horizon H_∞ consensus control problem for time-varying MASs. Specifically, a multi-Round-Robin protocol is adopted to schedule network resource allocation in the information exchange among neighboring agents. This work addresses three fundamental challenges: (1) how to appropriately model the scheduling behavior of the multi-Round-Robin protocol in communication processes between adjacent agents? (2) how to strike a balance between consensus control performance and the control effort as well as the observer correction effort of the agents? and (3) how to co-design an observer-based cooperative controller for time-varying MASs under external disturbances that fulfills the prescribed H_∞ performance requirement?

The primary objective of this paper is to address three key questions, with the main contributions summarized as follows:

1. Different from the existing consensus results developed under conventional Round-Robin scheduling protocols (e.g., [29, 30, 35]), this paper, for the first time, investigates the finite-horizon H_∞ consensus problem for discrete time-varying MASs under a multi-Round-Robin scheduling mechanism. A novel binary-matrix-based modeling approach is developed to effectively capture the scheduling behavior of the protocol and can be readily adapted to the conventional Round-Robin protocol.

2. To address the tradeoff between consensus regulation quality and implementation effort, a synthesis-oriented quadratic performance index is constructed, which simultaneously penalizes the consensus error, the control energy, and the observer correction energy. Compared with conventional performance indices (e.g., [14,40]), this formulation provides an explicit mechanism for balancing consensus performance, control actuation effort, and observer update effort within a unified design framework.
3. A novel design method based on two coupled backward recursive Riccati difference equations (RDEs) is established to simultaneously compute the observer and controller gains within the time-varying framework and achieve the desired H_∞ consensus performance. Compared to [39], this co-design strategy provides a systematic way to synthesize the observer-based consensus controller under the multi-Round-Robin scheduling mechanism.

The remainder of this paper is structured as follows. Section 2 introduces the necessary preliminaries, covering graph theory, the multi-Round-Robin protocol, and the problem formulation. In Section 3, sufficient conditions for achieving the H_∞ consensus performance are established, with the controller parameters and observer gains designed via two coupled backward recursive RDEs. A numerical example is provided in Section 4 to demonstrate the effectiveness of the proposed methodology. Finally, Section 5 presents concluding remarks and suggests potential directions for future research.

Notations: Unless otherwise stated, the notation used in this paper follows established conventions. $\mathbb{E}\{x\}$ denotes the expectation of the stochastic variable x. I denotes the identity matrix with appropriate dimensions when no confusion arises. $\mathrm{diag}\{\cdots\}$ represents a block-diagonal matrix. $\|x\|$ denotes the Euclidean norm of a vector x, and $|x|$ denotes the cardinality of the set x. For a matrix $M \in \mathbb{R}^{m\times n}$, $M^\dagger$ denotes its Moore-Penrose pseudo inverse. $\|M\|_F$ denotes the Frobenius norm of the matrix M. $\otimes$ and $\circ$ denote the Kronecker product and the Hadamard product of matrices, respectively. $\gcd(a,b)$ denotes the greatest common divisor of the integers a and b.

2. Preliminaries and problem formulation

2.1. Graph Theory

Consider a weighted directed graph $\mathcal{G}(\mathcal{V},\mathcal{E},\mathcal{H})$ with n nodes, where $\mathcal{V} \triangleq \{v_1, v_2, \ldots, v_n\}$ denotes the finite set of nodes, $\mathcal{E} \subseteq \mathcal{V}\times\mathcal{V}$ represents the set of directed edges, and $\mathcal{H} \triangleq [h_{i,j}]_{n\times n}$ with $0 \le h_{i,j} \le 1$ is the weighted adjacency matrix with non-negative elements. An edge $e_{ij} \triangleq (v_i, v_j) \in \mathcal{E}$ indicates a directed information flow from node v_j to its neighboring node v_i. The set of neighboring nodes of v_i is defined as $\mathcal{N}_i \triangleq \{v_j \in \mathcal{V} \mid (v_i, v_j) \in \mathcal{E}\}$. Let $\mathcal{D} \triangleq \mathrm{diag}\{d_1, d_2, \ldots, d_n\}$ be a diagonal matrix with $d_i \triangleq \sum_{j=1}^{n} h_{i,j}$.

2.2. System Description

Consider a discrete time-varying MAS defined over finite horizon $s \in [0, \tau-1]$. The MAS comprises n agents with node set $\mathcal{V} = \{1, 2, \ldots, n\}$. For each agent $i \in \mathcal{V}$, the dynamic model is described as follows:

$$\begin{cases} x_i(s+1) = A(s)x_i(s) + B(s)u_i(s) + E(s)w_i(s) \\ y_i(s) = C(s)x_i(s) + F(s)\nu_i(s) \\ z_i(s) = M(s)x_i(s) \end{cases} \tag{1}$$

where $x_i(s) \in \mathbb{R}^{n_x}$ and $u_i(s) \in \mathbb{R}^{n_u}$ denote the system state and the control input of agent i, respectively; $y_i(s) \in \mathbb{R}^{n_y}$ and $z_i(s) \in \mathbb{R}^{n_z}$ denote the measurement output and the controlled output of agent i, respectively; $w_i(s) \in l_2([0,\tau-1];\mathbb{R}^{n_\omega})$ and $\nu_i(s) \in l_2([0,\tau-1];\mathbb{R}^{n_\nu})$ denote the process disturbance and measurement disturbance, respectively. Matrices $A(s)$, $B(s)$, $C(s)$, $E(s)$, $F(s)$, and $M(s)$ are time-varying system parameters with appropriate dimensions.

It is assumed that the system state is unmeasurable. To enhance the robustness of the control method against external disturbances, observers are applied to estimate the internal state of each agent, which has the following form:

$$\begin{cases} \hat{x}_i(s+1) = A(s)\hat{x}_i(s) + B(s)u_i(s) + L(s)\big(y_i(s) \\ \qquad\qquad - C(s)\hat{x}_i(s)\big) \\ \hat{z}_i(s) = M(s)\hat{x}_i(s) \end{cases}$$

where $\hat{x}_i(s)$ and $\hat{z}_i(s)$ denote the estimated state and estimated controlled output of agent i, respectively, and $L(s)$ is the observer gain to be determined.

To ensure the solvability of the consensus control problem and facilitate the subsequent analysis, we give the following assumption regarding communication topology.

Assumption 1. *Ref.* [24]. *For the considered MAS in (1), the directed graph $\mathcal{G}$ contains a directed spanning tree.*

2.3. Multi-Round-Robin Protocol

To achieve consensus, each agent communicates with its neighbors over a shared network under a potentially time-varying topology. To efficiently manage network resources, prevent data collisions, and minimize bandwidth waste, a multi-Round-Robin protocol, inspired by [37], is introduced to regulate the transmission order among agents.

Under the multi-Round-Robin protocol, agent i can only receive data from a specifically selected subset of its neighbors during each transmission slot. The following proposition formalizes the multi-Round-Robin scheduling mechanism.

Proposition 1. *For agent i, let its ordered neighbor set be $\mathcal{N}_i = \{v_1, v_2, \ldots, v_{p_i}\}$, and let the multi-Round-Robin scheduling rule be defined by*

$$\zeta_i(s) \triangleq \{\kappa_{i,1}(s), \kappa_{i,2}(s), \ldots, \kappa_{i,\iota_i}(s)\}, \tag{2}$$

$$\kappa_{i,j}(s) \triangleq mod((s-1)\iota_i + j - 1,\ p_i) + 1, \quad j = 1, 2, \ldots, \iota_i, \tag{3}$$

where $\zeta_i(s)$ denotes the set of indices of the neighbors scheduled to transmit to agent i at time instant s. Then the above rule realizes a multi-Round-Robin scheduling mechanism in the following sense:

1. *at each time instant s, exactly ι_i distinct neighbors are selected;*
2. *the selected neighbors are consecutive in the fixed cyclic ordering of $\mathcal{N}_i$;*
3. *from time s to $s+1$, the selected set shifts forward by ι_i positions in the cyclic ordering;*
4. *the scheduling period is $T_i = p_i / \gcd(p_i, \iota_i)$.*

Proof. The following proof is organized into four main steps, each addressing one of the claims in the proposition.

First, for any $j \in \{1, 2, \ldots, \iota_i\}$, by the definition of the modulo operation,

$$0 \le \mathrm{mod}\big((s-1)\iota_i + j - 1,\ p_i\big) \le p_i - 1.$$

Hence, $1 \le \kappa_{i,j}(s) \le p_i$. Therefore, each $\kappa_{i,j}(s)$ is a valid index of the ordered neighbor set $\mathcal{N}_i$.

Second, we show that the selected indices are pairwise distinct. Consider any $j_1, j_2 \in \{1, 2, \ldots, \iota_i\}$ with $j_1 \ne j_2$. Suppose, by contradiction, that

$$\kappa_{i,j_1}(s) = \kappa_{i,j_2}(s).$$

Then, $\mathrm{mod}\big((s-1)\iota_i + j_1 - 1,\ p_i\big) = \mathrm{mod}\big((s-1)\iota_i + j_2 - 1,\ p_i\big)$, which implies $j_1 - j_2 \equiv 0 \pmod{p_i}$. However, since $j_1, j_2 \in \{1, 2, \ldots, \iota_i\}$ and $\iota_i < p_i$, one has

$$0 < |j_1 - j_2| < p_i,$$

and thus $j_1 - j_2$ cannot be a multiple of p_i, which is a contradiction. Therefore, $\kappa_{i,1}(s), \kappa_{i,2}(s), \ldots, \kappa_{i,\iota_i}(s)$ are pairwise distinct, and consequently, $|\zeta_i(s)| = \iota_i$. This proves that exactly ι_i neighbors are selected at each time instant.

Third, we prove that these selected neighbors are consecutive in the cyclic ordering and that the set shifts forward by ι_i positions at the next time instant. For any fixed s and any $j \in \{1, 2, \ldots, \iota_i - 1\}$, one has

$$\kappa_{i,j+1}(s) = \mathrm{mod}\big((s-1)\iota_i + j - 1,\ p_i\big) + 1.$$

Hence, compared with $\kappa_{i,j}(s)$, the index increases by one position in the cyclic ordering modulo p_i. Therefore, the selected indices in $\zeta_i(s)$ form ι_i consecutive positions on the cycle $1 \to 2 \to \cdots \to p_i \to 1$.

Moreover,

$$\begin{aligned} \kappa_{i,j}(s+1) &= \mathrm{mod}\big(s\iota_i + j - 1,\ p_i\big) + 1 \\ &= \mathrm{mod}\big(\kappa_{i,j}(s) + \iota_i,\ p_i\big) + 1. \end{aligned}$$

Thus, each selected index at time $s+1$ is obtained from the corresponding selected index at time s by shifting forward ι_i positions modulo p_i. Therefore, the selected neighbor set evolves cyclically by a step size of ι_i, which is exactly the defining feature of a multi-Round-Robin mechanism.

Finally, we determine the period. The scheduling returns to its initial configuration if and only if the starting position of the selected block returns to its initial value. This is equivalent to the existence of a positive integer T_i such that $T_i\iota_i \equiv 0 \pmod{p_i}$. The smallest positive integer satisfying the above congruence is well known to be $T_i = p_i/\gcd(p_i, \iota_i)$. Hence, the scheduling rule is periodic with period T_i.

Combining the above four steps, we conclude that the defined rule indeed realizes a multi-Round-Robin scheduling mechanism. □

To simplify the description, a mapping function $\mathscr{M}(\cdot)$ is introduced to convert the set $\zeta_i(s)$ representing selected neighbors into a vector comprising binary values, which characterizes the scheduling behavior of the multi-Round-Robin protocol. Specifically, for agent i with neighbor set $\mathcal{N}_i \triangleq \{v_1, v_2, \ldots, v_{p_i}\}$, where v_k ($k \in \{1, 2, \ldots, p_i\}$) denotes the k-th neighbor of agent i in a fixed ordering, the mapping function $\mathscr{M}(\cdot)$ is defined as:

$$\mathscr{M}(\zeta_i(s)) \triangleq \vec{\chi}_i(s) \triangleq [\chi_{i,1}(s), \chi_{i,2}(s), \ldots, \chi_{i,n}(s)]^T,$$
$$\chi_{i,j}(s) = \begin{cases} 1, & \text{if } j \in \mathcal{N}_i \text{ and } \exists k \in \zeta_i(s) \text{ such that } j = v_k \\ 0, & \text{otherwise} \end{cases}$$

where $\chi_{i,j}(s)$ denotes the j-th element of $\vec{\chi}_i(s)$, indicating whether agent j is selected to transmit information to agent i at time instant s.

The global scheduling behavior of the multi-Round-Robin protocol is characterized by the following matrix:

$$\Lambda(s) \triangleq [\vec{\chi}_1(s), \vec{\chi}_2(s), \ldots, \vec{\chi}_n(s)]^T. \tag{4}$$

Remark 1. *To illustrate the effectiveness of the specially designed representation method, we give the following example. Consider agent i with $p_i = 5$ neighbors, where $\mathcal{N}_i = \{2, 4, 7, 9, 11\}$ (i.e., $v_1 = 2$, $v_2 = 4$, $v_3 = 7$, $v_4 = 9$, $v_5 = 11$) and $\iota_i = 2$. At time s, since $\iota_i = 2$, the multi-Round-Robin protocol selects two neighbors, yielding $\zeta_i(s) = \{2, 3\}$ (i.e., $\kappa_{i,1}(s) = 2$ and $\kappa_{i,2}(s) = 3$). Then, $\chi_{i,j}(s) = 1$ for $j \in \{4, 7\}$ because:*

- *For $j = 4$: $4 \in \mathcal{N}_i$ and $4 = v_2$, where $k = 2 = \kappa_{i,1}(s) \in \zeta_i(s)$.*
- *For $j = 7$: $7 \in \mathcal{N}_i$ and $7 = v_3$, where $k = 3 = \kappa_{i,2}(s) \in \zeta_i(s)$.*

For all other agents $j \notin \{4, 7\}$, we have $\chi_{i,j}(s) = 0$.

Remark 2. *The scheduling behavior of the multi-Round-Robin protocol is illustrated in Figure 1. Each colored block represents a distinct neighboring agent. In this example, agents i, j, and k have 3, 4, and 5 neighbors, respectively, implying $p_i = 3$, $p_j = 4$, and $p_k = 5$. As time progresses, the selected neighbors cycle sequentially. When $\iota_i = 1$, $\iota_j = 2$, and $\iota_k = 2$, the scheduling period for agent i is T_i, completing one full cycle. Taking agent j as an example: at time $s = 1$, it selects the adjacent agents denoted by the blue and green block; at time $s = 2$, its selection shifts to those marked by yellow and red block. These two consecutive time steps constitute one complete scheduling cycle for agent j. It is worth pointing out that, when $\iota_i = 1$ for each agent, the multi-Round-Robin protocol reduces to the conventional Round-Robin protocol.*

Remark 3. *Unlike conventional protocol modeling methods, where the scheduling behavior is usually described by a mode-dependent switched system model (see [41,42]), the proposed binary scheduling matrix directly characterizes the activation status of all communication edges at each transmission instant. Such a representation is particularly suitable for the multi-Round-Robin protocol, where multiple neighboring agents may be scheduled simultaneously. It avoids cumbersome mode enumeration, and leads to a compact closed-loop formulation for the subsequent RDE-based controller and observer design.*

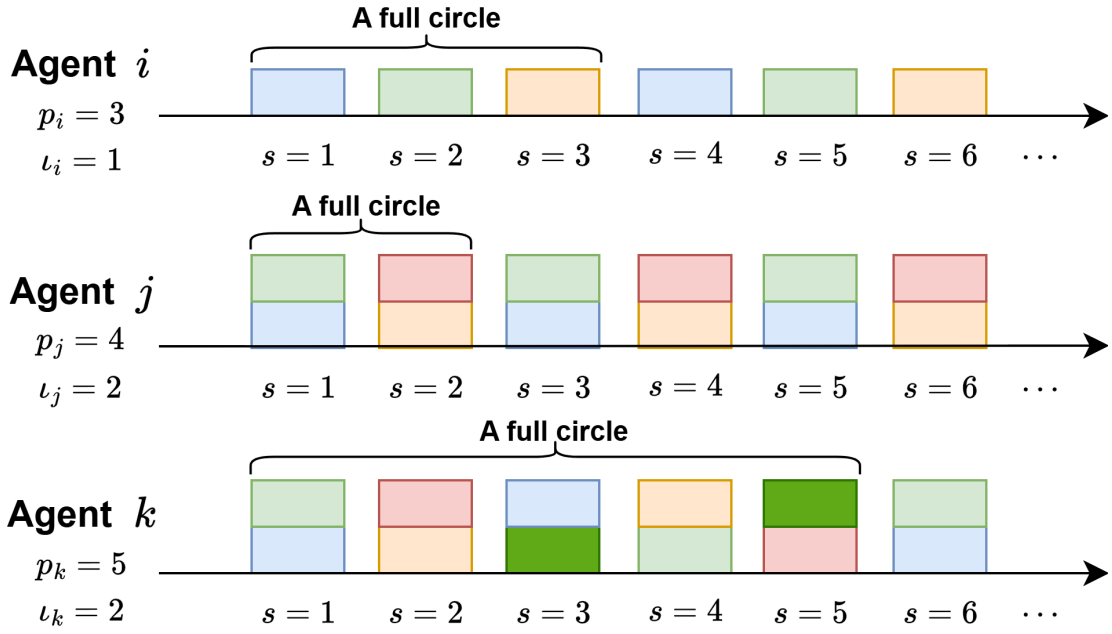

Figure 1. An example for the multi-Round-Robin protocol scheduling.

2.4. Augmentation Error System

Before preceding, we introduce the following lemma, which will be used in the subsequent analysis.

Lemma 1. *Ref.* [43]. *For any matrices $\mathcal{A}$, $\mathcal{B}$, $\mathcal{C}$ and $\mathcal{D}$ with appropriate dimensions, the Kronecker product $\otimes$ satisfies:*

1. $(\mathcal{A}+\mathcal{B})\otimes\mathcal{C} = \mathcal{A}\otimes\mathcal{C}+\mathcal{B}\otimes\mathcal{C}$.
2. $(\mathcal{A}\otimes\mathcal{B})(\mathcal{C}\otimes\mathcal{D}) = (\mathcal{AC})\otimes(\mathcal{BD})$.
3. $(\mathcal{A}\otimes\mathcal{B})^T = \mathcal{A}^T\otimes\mathcal{B}^T$.
4. $(\mathcal{A}\otimes\mathcal{B})^{-1} = \mathcal{A}^{-1}\otimes\mathcal{B}^{-1}$, *if* $\mathcal{A}^{-1}$ *and* $\mathcal{B}^{-1}$ *exist.*

Lemma 2. *Ref.* [14]. *Let $\mathcal{A}$, $\mathcal{B}$ and $\mathcal{C}$ be known nonzero matrices with appropriate dimensions. The solution $\mathcal{X}$ to $\min_{\mathcal{X}}\|\mathcal{AXC}-\mathcal{B}\|_F$ is $\mathcal{A}^{\dagger}\mathcal{BC}^{\dagger}$.*

Based on the multi-Round-Robin scheduling and state estimation, the consensus controller for each agent is designed as

$$u_i(s) = K(s)\sum_{j=1}^{n}\chi_{i,j}(s)h_{i,j}\big(\hat{x}_j(s)-\hat{x}_i(s)\big) \tag{5}$$

where $u_i(s)$ $(i\in\mathcal{V})$ denotes the control input of agent i, $K(s)\in\mathbb{R}^{n_u\times n_x}$ $(s\in[0,\tau-1])$ is the feedback gain matrix to be determined.

Based on the introduced auxiliary matrix $\Lambda(s)$, controller (5) is rewritten by

$$u_i(s) = K(s)\sum_{j=1}^{n}h_{i,j}\lambda_{i,j}(s)\big(\hat{x}_j(s)-\hat{x}_i(s)\big) \tag{6}$$

where $\lambda_{i,j}(s)$ denotes the (i,j)-th entry of matrix $\Lambda(s)$. $\lambda_{i,j}(s)\in 0,1$ acts as a scheduling gate for edge $(j\to i)$: $\lambda_{i,j}(s)=1$ if neighbor j is selected by the multi-Round-Robin protocol at time s, and $\lambda_{i,j}(s)=0$ otherwise.

The state consensus error and controlled output consensus error are defined as follows:

$$\begin{cases}\bar{x}_i(s)\triangleq\hat{x}_i(s)-(1/n)\sum_{j=1}^{n}\hat{x}_j(s)\\ \bar{z}_i(s)\triangleq\hat{z}_i(s)-(1/n)\sum_{j=1}^{n}\hat{z}_j(s).\end{cases} \tag{7}$$

To facilitate the subsequent analysis, the following vectors are defined:

$$\begin{aligned}
x(s) &\triangleq \begin{bmatrix} x_1^T(s) & x_2^T(s) & \dots & x_n^T(s) \end{bmatrix}^T, \\
y(s) &\triangleq \begin{bmatrix} y_1^T(s) & y_2^T(s) & \dots & y_n^T(s) \end{bmatrix}^T, \\
z(s) &\triangleq \begin{bmatrix} z_1^T(s) & z_2^T(s) & \dots & z_n^T(s) \end{bmatrix}^T, \\
\hat{x}(s) &\triangleq \begin{bmatrix} \hat{x}_1^T(s) & \hat{x}_2^T(s) & \dots & \hat{x}_n^T(s) \end{bmatrix}^T, \\
\hat{z}(s) &\triangleq \begin{bmatrix} \hat{z}_1^T(s) & \hat{z}_2^T(s) & \dots & \hat{z}_n^T(s) \end{bmatrix}^T, \\
u(s) &\triangleq \begin{bmatrix} u_1^T(s) & u_2^T(s) & \dots & u_n^T(s) \end{bmatrix}^T, \\
w(s) &\triangleq \begin{bmatrix} w_1^T(s) & w_2^T(s) & \dots & w_n^T(s) \end{bmatrix}^T, \\
\nu(s) &\triangleq \begin{bmatrix} \nu_1^T(s) & \nu_2^T(s) & \dots & \nu_n^T(s) \end{bmatrix}^T.
\end{aligned}$$

From (5), it is deduced that

$$u(s) = \big(\mathcal{H}_\phi(s) \otimes K(s)\big)\hat{x}(s) \tag{8}$$

where $\mathcal{H}_\phi(s) \triangleq \mathcal{H} \circ \Lambda(s) - \mathcal{D}$, with $\mathcal{D} = \text{diag}\{d_1, d_2, \dots, d_n\}$ and $d_i = \sum_{j=1}^n h_{i,j}\lambda_{i,j}(s)$.

Based on Lemma 1, the following global system is obtained:

$$\begin{cases}
x(s+1) = \big(I_n \otimes A(s)\big)x(s) + \big(I_n \otimes B(s)\big)u(s) \\
\qquad\qquad + \big(I_n \otimes E(s)\big)w(s) \\
y(s) = \big(I_n \otimes C(s)\big)x(s) + \big(I_n \otimes F(s)\big)\nu(s) \\
z(s) = \big(I_n \otimes M(s)\big)x(s).
\end{cases}$$

From (2), it is deduced that

$$\begin{aligned}
\hat{x}(s+1) = &\big(I_n \otimes A(s) + \mathcal{H}_\phi(s) \otimes (B(s)K(s))\big)\hat{x}(s) \\
&+ \big(I_n \otimes (L(s)C(s))\big)\big(x(s) - \hat{x}(s)\big) \\
&+ \big(I_n \otimes (L(s)F(s))\big)\nu(s).
\end{aligned}$$

Define $\bar{x}(s) \triangleq [\bar{x}_1^T(s) \quad \bar{x}_2^T(s) \quad \dots \quad \bar{x}_n^T(s)]^T$ and $\bar{z}(s) \triangleq [\bar{z}_1^T(s) \quad \bar{z}_2^T(s) \quad \dots \quad \bar{z}_n^T(s)]^T$. It is derived from (7) that

$$\begin{cases}
\bar{x}(s) = (\mathscr{F} \otimes I_{n_x})\hat{x}(s) \\
\bar{z}(s) = (\mathscr{F} \otimes I_{n_z})\hat{z}(s)
\end{cases} \tag{9}$$

where $\mathscr{F} \triangleq I_n - (1/n)\mathbf{1}_n\mathbf{1}_n^T$;

Defining the estimation error as $e(s) \triangleq x(s) - \hat{x}(s)$ and noting that $\mathcal{H}_\phi(s)\mathscr{F} = \mathcal{H}_\phi(s)$, one obtains

$$\begin{cases}
\bar{x}(s+1) = \big(I_n \otimes A(s) + (\mathscr{F}\mathcal{H}_\phi(s)) \otimes (B(s)K(s))\big) \\
\qquad\qquad \times \bar{x}(s) + \big(\mathscr{F} \otimes (L(s)C(s))\big)e(s) \\
\qquad\qquad + \big(\mathscr{F} \otimes (L(s)F(s))\big)\nu(s) \\
e(s+1) = \big(I_n \otimes A(s) - I_n \otimes (L(s)C(s))\big)e(s) \\
\qquad\qquad + \big(I_n \otimes E(s)\big)w(s) - \big(I_n \otimes (L(s)F(s))\big)\nu(s).
\end{cases}$$

By denoting the augmented vector $\xi(s) \triangleq [\bar{x}^T(s) \quad e^T(s)]^T$ and $\bar{w}(s) \triangleq [w^T(s) \quad \nu^T(s)]^T$, the augmented closed-loop system is represented in the following form:

$$\begin{cases}
\xi(s+1) = \bar{A}(s)\xi(s) + \bar{D}(s)\bar{w}(s) \\
\bar{z}(s) = \bar{M}(s)\xi(s)
\end{cases} \tag{10}$$

where

$$\bar{A}(s) \triangleq \begin{bmatrix} \bar{A}_{11}(s) & \bar{A}_{12}(s) \\ \mathbf{0} & \bar{A}_{22}(s) \end{bmatrix}, \bar{D}(s) \triangleq \begin{bmatrix} \mathbf{0} & \bar{D}_{12}(s) \\ \bar{D}_{21}(s) & \bar{D}_{22}(s) \end{bmatrix},$$
$$\bar{M}(s) \triangleq [I_n \otimes M(s) \quad \mathbf{0}],\ \bar{A}_{12}(s) \triangleq \mathscr{F} \otimes (L(s)C(s)),$$
$$\bar{A}_{11}(s) \triangleq I_n \otimes A(s) + (\mathscr{F}\mathcal{H}_\phi(s)) \otimes (B(s)K(s)),$$
$$\bar{D}_{22}(s) \triangleq -I_n \otimes (L(s)F(s)),$$
$$\bar{A}_{22}(s) \triangleq I_n \otimes \big(A(s) - (L(s)C(s))\big),$$
$$\bar{D}_{12}(s) \triangleq \mathscr{F} \otimes (L(s)F(s)), \quad \bar{D}_{21}(s) \triangleq I_n \otimes E(s).$$

Before proceeding, the following definition is introduced.

Definition 1. *Ref.* [14]. *The considered MAS (1) is said to meet the H_∞ consensus performance requirement over the finite-horizon $[0, \tau - 1]$, if the following condition is satisfied:*

$$J_1 \triangleq \sum_{i=1}^{n}\sum_{s=0}^{\tau-1}\Big(\|\bar{z}_i(s)\|^2 - \gamma^2\Big(\|w_i(s)\|^2 + \|\nu_i(s)\|^2\Big)\Big) - \gamma^2 \sum_{i=1}^{n} \bar{x}_i^T(0) W \bar{x}_i(0) < 0 \tag{11}$$

for $\forall\big(w_i(s), \nu_i(s), \bar{x}_i(0)\big) \neq 0$, where $\gamma > 0$ is a specified disturbance attenuation level, and $W = W^T > 0$ is a given positive definite matrix.

The objective of this paper is to design an observer-based consensus controller for MAS (1) under a multi-Round-Robin protocol scheduling, such that the extended dynamics (10) satisfies the following reformulated H_∞ performance constraint:

$$\sum_{s=0}^{\tau-1}\Big(\|\bar{z}(s)\|^2 - \gamma^2\|\bar{w}(s)\|^2\Big) - \gamma^2 \xi^T(0)\mathcal{W}\xi(0) < 0 \tag{12}$$

where $\mathcal{W} = \text{diag}\{I_n \otimes W, \mathbf{0}\}$.

3. Main Result

The following theorem is given for the analysis of the H_∞ performance of the MAS.

Theorem 1. *Consider time-varying MAS (10) under the multi-Round-Robin scheduling. Given the disturbance attenuation level $\gamma > 0$, the controller gain matrices $\{K(s)\}_{s\in[0,\tau-1]}$, the observer gain matrices $\{L(s)\}_{s\in[0,\tau-1]}$, and the positive definite matrix W, the system (10) achieves the H_∞ performance criterion (12) if there exist a sequence of non-negative definite matrices $\{\mathcal{P}(s)\}_{s\in[0,\tau-1]}$ satisfying the following backward recursive RDE:*

$$\mathcal{P}(s) = \bar{A}^T(s)\mathcal{P}(s+1)\bar{A}(s) + \bar{M}^T(s)\bar{M}(s) + \bar{A}^T(s) \times \mathcal{P}(s+1)\bar{D}(s)\Delta^{-1}(s)\bar{D}^T(s)\mathcal{P}(s+1)\bar{A}(s) \tag{13}$$

subject to

$$\begin{cases} \mathcal{P}(0) \leq \gamma^2\mathcal{W} \\ \mathcal{P}(\tau) = 0 \\ \Delta(s) \triangleq \gamma^2 I - \bar{D}^T(s)\mathcal{P}(s+1)\bar{D}(s) > 0. \end{cases} \tag{14}$$

Proof. Define $V_1(s) \triangleq \xi^T(s)\mathcal{P}(s)\xi(s)$. Then, one obtains that

$$\begin{aligned}\mathscr{Y}_1(s) &\triangleq V_1(s+1) - V_1(s)\\ &= \xi^T(s)\big(\bar{A}^T(s)\mathcal{P}(s+1)\bar{A}(s) - \mathcal{P}(s)\big)\xi(s) + \xi^T(s)\\ &\quad \times \bar{A}^T(s)\mathcal{P}(s+1)\bar{D}(s)\bar{w}(s) + \bar{w}^T(s)\bar{D}^T(s)\\ &\quad \times \mathcal{P}(s+1)\bar{A}(s)\xi(s) + \bar{w}^T(s)\bar{D}^T(s)\mathcal{P}(s+1)\\ &\quad \times \bar{D}(s)\bar{w}(s).\end{aligned}$$

Adding the following zero term to the equation:

$$\|\bar{z}(s)\|^2 - \gamma^2\|\bar{w}(s)\|^2 - \|\bar{z}(s)\|^2 + \gamma^2\|\bar{w}(s)\|^2 = 0,$$

one obtains

$$\begin{aligned}\mathscr{Y}_1(s) &= \xi^T(s)\big(\bar{A}^T(s)\mathcal{P}(s+1)\bar{A}(s) + \bar{M}^T(s)\bar{M}(s)\big)\xi(s)\\ &\quad + \xi^T(s)\bar{A}^T(s)\mathcal{P}(s+1)\bar{D}(s)\bar{w}(s) + \bar{w}^T(s)\bar{D}^T(s)\\ &\quad \times \mathcal{P}(s+1)\bar{A}(s)\xi(s) + \bar{w}^T(s)\big(\bar{D}^T(s)\mathcal{P}(s+1)\\ &\quad \times \bar{D}(s) - \gamma^2 I\big)\bar{w}(s) - \xi^T(s)\mathcal{P}(s)\xi(s) - \|\bar{z}(s)\|^2\\ &\quad + \gamma^2\|\bar{w}(s)\|^2.\end{aligned}$$

Utilizing the completing squares method and according to (13), we obtain

$$\begin{aligned}\mathscr{Y}_1(s) = &-\big(\bar{w}(s) - w^*(s)\big)^T\Delta(s)\big(\bar{w}(s) - w^*(s)\big)\\ &- \|\bar{z}(s)\|^2 + \gamma^2\|\bar{w}(s)\|^2\end{aligned} \tag{15}$$

where $w^*(s) \triangleq \Delta^{-1}(s)\bar{D}^T(s)\mathcal{P}(s+1)\bar{A}(s)\xi(s)$.

Summing both sides of (15) from 0 to $\tau - 1$, it follows that

$$\begin{aligned}\xi^T(\tau)\mathcal{P}(\tau)\xi(\tau) = &\ \xi^T(0)\mathcal{P}(0)\xi(0)\\ &+ \sum_{s=0}^{\tau-1} -\big(\bar{w}(s) - w^*(s)\big)^T\Delta(s)\big(\bar{w}(s) - w^*(s)\big)\\ &- \sum_{s=0}^{\tau-1}\big(\|\bar{z}(s)\|^2 - \gamma^2\|\bar{w}(s)\|^2\big).\end{aligned}$$

Since $\Delta(s) > 0$, $\mathcal{P}(0) \le \gamma^2\mathcal{W}$, and $\mathcal{P}(\tau) = 0$, one has

$$\begin{aligned}J_1 = &-\sum_{s=0}^{\tau-1}\big(\bar{w}(s) - w^*(s)\big)^T\Delta(s)\big(\bar{w}(s) - w^*(s)\big)\\ &+ \xi^T(0)\big(\mathcal{P}(0) - \gamma^2\mathcal{W}\big)\xi(0) < 0\end{aligned}$$

which implies that the predefined H_∞ performance criterion (12) is satisfied. The proof is complete. □

So far, we have established the sufficient conditions regarding the predefined H_∞ performance criterion with the specified disturbance attenuation level γ and the positive definite matrix W. In what follows, we proceed to design the controller gain matrices $K(s)$ and the observer gain matrices $L(s)$ under the worst-case disturbance scenario, i.e., when $\bar{w}(s) = w^*(s)$.

Based on (8) and (9), and to facilitate the subsequent analysis, define $\tilde{y}(s) \triangleq (I_n \otimes C(s))e(s)$. Then, it is deduced that

$$\begin{cases} u(s) = \bar{K}(s)\xi(s)\\ \tilde{y}(s) = \tilde{C}(s)\xi(s)\end{cases} \tag{16}$$

where

$$\bar{K}(s) \triangleq \begin{bmatrix}\mathcal{H}_\phi(s) \otimes K(s) & \mathbf{0}\end{bmatrix},\ \tilde{C}(s) \triangleq \begin{bmatrix}\mathbf{0} & I_n \otimes C(s)\end{bmatrix}.$$

The closed-loop system (10) is rewritten as follows:

$$\begin{cases} \xi(s+1) = \big(\tilde{A}(s) + \tilde{D}(s)\big)\xi(s) + \tilde{B}(s)u(s) + \bar{L}(s)\tilde{y}(s) \\ \bar{z}(s) = \bar{M}(s)\xi(s) \end{cases} \tag{17}$$

where

$$\begin{aligned} &\tilde{A}(s) \triangleq \begin{bmatrix} I_n \otimes A(s) & \mathbf{0} \\ \mathbf{0} & I_n \otimes A(s) \end{bmatrix}, \\ &\tilde{B}(s) \triangleq \begin{bmatrix} \mathscr{F} \otimes B(s) \\ \mathbf{0} \end{bmatrix}, \bar{L}(s) \triangleq \begin{bmatrix} \mathscr{F} \otimes L(s) \\ I_n \otimes L(s) \end{bmatrix}, \\ &\tilde{D}(s) \triangleq \bar{D}(s)\Delta^{-1}(s)\bar{D}^T(s)\mathcal{P}(s+1)\bar{A}(s). \end{aligned} \tag{18}$$

In this paper, a quadratic cost function is introduced in accordance with the standard optimal control rationale to balance regulation performance and implementation effort.

The cost function is defined as

$$J_2 \triangleq \sum_{s=0}^{\tau-1} \Big(\|\bar{z}(s)\|^2 + \varepsilon_1 \|u(s)\|^2 + \varepsilon_2 \|\bar{L}(s)\tilde{y}(s)\|^2 \Big) \tag{19}$$

where $\varepsilon_1 > 0$ and $\varepsilon_2 > 0$ are given constants. Specifically, the term $\|\bar{z}(s)\|^2$ penalizes the consensus error and therefore directly reflects the control objective; the term $\varepsilon_1\|u(s)\|^2$ penalizes the control energy to prevent excessively aggressive actuation; and the term $\varepsilon_2\|\bar{L}(s)\tilde{y}(s)\|^2$ penalizes the observer correction energy so as to avoid overly large observer gains and excessive sensitivity to measurement innovation. Therefore, J_2 is introduced as a synthesis-oriented quadratic performance index under the H_∞ robustness constraint induced by J_1.

Based on Theorem 1, we now proceed to design the controller gain matrices and observer gain matrices such that the system achieves the H_∞ performance constraint.

Theorem 2. *Consider the time-varying MAS (17) under the multi-Round-Robin scheduling. Given the positive scalars $\varepsilon_1 > 0$, $\varepsilon_2 > 0$ and the positive definite matrix W, there exist controller gain matrices $\{K(s)\}_{s\in[0,\tau-1]}$ and observer gain matrices $\{L(s)\}_{s\in[0,\tau-1]}$ for the cooperative controllers and the state observer, respectively, such that the system (17) satisfies the H_∞ performance constraint (19), if there exist solutions $\{\mathcal{Q}(s), \bar{K}(s), \bar{L}(s)\}_{s\in[0,\tau-1]}$ satisfying the RDE (13) and the following backward recursive RDE:*

$$\begin{aligned} \mathcal{Q}(s) = &\big(\tilde{A}(s) + \tilde{D}(s)\big)^T \mathcal{Q}(s+1)\big(\tilde{A}(s) + \tilde{D}(s)\big) - \tilde{A}^T(s) \\ &\times \mathcal{Q}(s+1)\tilde{B}(s)\nabla_1^{-1}(s)\tilde{B}^T(s)\mathcal{Q}(s+1)\tilde{A}(s) \\ &- \tilde{A}^T(s)\mathcal{Q}(s+1)\nabla_2^{-1}(s)\mathcal{Q}(s+1)\tilde{A}(s) + \bar{K}^T(s) \\ &\times \tilde{B}^T(s)\mathcal{Q}(s+1)\tilde{D}(s) + \bar{M}^T(s)\bar{M}(s) + \bar{K}^T(s) \\ &\times \tilde{B}^T(s)\mathcal{Q}(s+1)\bar{L}(s)\tilde{C}(s) + \tilde{D}^T(s)\mathcal{Q}(s+1) \\ &\times \bar{L}(s)\tilde{C}(s) \end{aligned} \tag{20}$$

subject to

$$\begin{cases} \mathcal{Q}(\tau) = 0 \\ \nabla_1(s) \triangleq \tilde{B}^T(s)\mathcal{Q}(s+1)\tilde{B}(s) + \varepsilon_1 I > 0 \\ \nabla_2(s) \triangleq \mathcal{Q}(s+1) + \varepsilon_2 I > 0 \end{cases}$$

with the gains-related matrices being designed as follows:

$$\begin{cases} \bar{K}(s) = -\mathcal{U}(s) \\ \bar{L}(s) = -\mathcal{T}(s)\tilde{C}^\dagger(s) \end{cases} \tag{21}$$

where

$$\begin{aligned}\mathcal{U}(s) &\triangleq \nabla_1^{-1}(s)\tilde{B}^T(s)\mathcal{Q}(s+1)\tilde{A}(s),\\ \mathcal{T}(s) &\triangleq \nabla_2^{-1}(s)\mathcal{Q}(s+1)\tilde{A}(s)\end{aligned} \tag{22}$$

Proof. Define $V_2(s) \triangleq \xi^T(s)\mathcal{Q}(s)\xi(s)$. Then, one obtains that

$$\begin{aligned}\mathscr{Y}_2(s) &\triangleq V_2(s+1) - V_2(s)\\ &= \xi^T(s)\Big(\big(\tilde{A}(s)+\tilde{D}(s)\big)^T\mathcal{Q}(s+1)\big(\tilde{A}(s)+\tilde{D}(s)\big)\\ &\quad - \mathcal{Q}(s)\Big)\xi(s) + u^T(s)\tilde{B}^T(s)\mathcal{Q}(s+1)\tilde{B}(s)u(s)\\ &\quad + \tilde{y}^T(s)\bar{L}^T(s)\mathcal{Q}(s+1)\bar{L}(s)\tilde{y}(s) + \tilde{y}^T(s)\bar{L}^T(s)\\ &\quad \times \mathcal{Q}(s+1)\tilde{A}(s)\xi(s) + \tilde{y}^T(s)\bar{L}^T(s)\mathcal{Q}(s+1)\\ &\quad \times \tilde{D}(s)\xi(s) + \tilde{y}^T(s)\bar{L}^T(s)\mathcal{Q}(s+1)\tilde{B}(s)u(s)\\ &\quad + u^T(s)\tilde{B}^T(s)\mathcal{Q}(s+1)\tilde{A}(s)\xi(s) + u^T(s)\tilde{B}^T(s)\\ &\quad \times \mathcal{Q}(s+1)\tilde{D}(s)\xi(s) + u^T(s)\tilde{B}^T(s)\mathcal{Q}(s+1)\\ &\quad \times \bar{L}(s)\tilde{y}(s) + \xi^T(s)\big(\tilde{A}(s)+\tilde{D}(s)\big)^T\mathcal{Q}(s+1)\\ &\quad \times \tilde{B}(s)u(s) + \xi^T(s)\big(\tilde{A}(s)+\tilde{D}(s)\big)^T\mathcal{Q}(s+1)\\ &\quad \times \bar{L}(s)\tilde{y}(s).\end{aligned}$$

Similar to the proof of Theorem 1, by adding the following zero term:

$$\begin{aligned}&\|\bar{z}(s)\|^2 + \varepsilon_1\|u(s)\|^2 + \varepsilon_2\|\bar{L}(s)\tilde{y}(s)\|^2\\ &- \|\bar{z}(s)\|^2 - \varepsilon_1\|u(s)\|^2 - \varepsilon_2\|\bar{L}(s)\tilde{y}(s)\|^2 = 0,\end{aligned}$$

and utilizing the completing squares method, one obtains

$$\begin{aligned}\mathscr{Y}_2(s) &= \xi^T(s)\Big(\big(\tilde{A}(s)+\tilde{D}(s)\big)^T\mathcal{Q}(s+1)\big(\tilde{A}(s)+\tilde{D}(s)\big)\\ &\quad - \tilde{A}^T(s)\mathcal{Q}(s+1)\tilde{B}(s)\nabla_1^{-1}(s)\tilde{B}^T(s)\mathcal{Q}(s+1)\tilde{A}(s)\\ &\quad - \tilde{A}^T(s)\mathcal{Q}(s+1)\nabla_2^{-1}(s)\mathcal{Q}(s+1)\tilde{A}(s) + \bar{K}^T(s)\\ &\quad \times \tilde{B}^T(s)\mathcal{Q}(s+1)\bar{L}(s)\tilde{C}(s) + \tilde{D}^T(s)\mathcal{Q}(s+1)\bar{L}(s)\\ &\quad \times \tilde{C}(s) - \mathcal{Q}(s) + \bar{K}^T(s)\tilde{B}^T(s)\mathcal{Q}(s+1)\tilde{D}(s)\\ &\quad + \bar{M}^T(s)\bar{M}(s)\Big)\xi(s) + \big(u(s)+u^*(s)\big)^T\nabla_1(s)\\ &\quad \times \big(u(s)+u^*(s)\big) + \big(\bar{L}(s)\tilde{y}(s)+y^*(s)\big)^T\nabla_2(s)\\ &\quad \times \big(\bar{L}(s)\tilde{y}(s)+y^*(s)\big) - \|\bar{z}(s)\|^2 - \varepsilon_1\|u(s)\|^2\\ &\quad - \varepsilon_2\|\bar{L}(s)\tilde{y}(s)\|^2.\end{aligned}$$

Based on (20), one deduces

$$\begin{aligned}\mathscr{Y}_2(s) &= \big(u(s)+u^*(s)\big)^T\nabla_1(s)\big(u(s)+u^*(s)\big)\\ &\quad + \big(\bar{L}(s)\tilde{y}(s)+y^*(s)\big)^T\nabla_2(s)\big(\bar{L}(s)\tilde{y}(s)+y^*(s)\big)\\ &\quad - \|\bar{z}(s)\|^2 - \varepsilon_1\|u(s)\|^2 - \varepsilon_2\|\bar{L}(s)\tilde{y}(s)\|^2\end{aligned} \tag{23}$$

where

$$\begin{cases} u^*(s) \triangleq \nabla_1^{-1}(s)\tilde{B}^T(s)\mathcal{Q}(s+1)\tilde{A}(s)\xi(s)\\ \qquad\quad = \mathcal{U}(s)\xi(s)\\ y^*(s) \triangleq \nabla_2^{-1}(s)\mathcal{Q}(s+1)\tilde{A}(s)\xi(s)\\ \qquad\quad = \mathcal{T}(s)\xi(s).\end{cases}$$

Summing both sides of (23) from 0 to $\tau-1$ with $\mathcal{Q}(\tau)=0$, it follows that

$$\begin{aligned}J_2=&\sum_{s=0}^{\tau-1}\Big(\big(u(s)+u^*(s)\big)^T\nabla_1(s)\big(u(s)+u^*(s)\big)\Big)\\&+\sum_{s=0}^{\tau-1}\Big(\big(\bar{L}(s)\tilde{y}(s)+y^*(s)\big)^T\nabla_2(s)\big(\bar{L}(s)\tilde{y}(s)+y^*(s)\big)\Big)\\&+\xi^T(0)\mathcal{Q}(0)\xi(0)\\\leq&\sum_{s=0}^{\tau-1}\Big(\|\bar{K}(s)+\mathcal{U}(s)\|_F^2\|\xi(s)\|^2\Big)+\xi^T(0)\mathcal{Q}(0)\xi(0)\\&+\sum_{s=0}^{\tau-1}\Big(\|\bar{L}(s)\tilde{C}(s)+\mathcal{T}(s)\|_F^2\|\xi(s)\|^2\Big).\end{aligned}$$

To minimize the cost function (19), $\bar{K}(s)$ and $\bar{L}(s)$ are chosen iteratively in a backward manner as follows:

$$\begin{cases}\bar{K}(s)=\underset{\bar{K}(s)}{\operatorname{argmin}}\|\bar{K}(s)+\mathcal{U}(s)\|_F\\\bar{L}(s)=\underset{\bar{L}(s)}{\operatorname{argmin}}\|\bar{L}(s)\tilde{C}(s)+\mathcal{T}(s)\|_F.\end{cases}$$

By means of Lemma 2, $\bar{K}(s)$ and $\bar{L}(s)$ are solved as (21). Subsequently, according to (16) and (18), and based on the properties of the Kronecker product, performing block extraction on the matrices $\bar{K}(s)$ and $\bar{L}(s)$, the controller gain matrices $K(s)$ and the observer gain matrices $L(s)$ can be calculated. The calculation procedure is straightforward and thus omitted here for brevity. □

In summary, based on the main results in the aforementioned theorems, we give the following Algorithm 1 to achieve finite-horizon H_∞ consensus control problem.

Algorithm 1: Observer-Based Finite-Horizon H_∞ Consensus Control

Step 1. Given the positive definite matrix W and the positive scalars γ, ε_1, and ε_2, set $s=\tau-1$, $\mathcal{P}(\tau)=0$, and $\mathcal{Q}(\tau)=0$.

Step 2. Calculate $\nabla_1(s)$ and $\nabla_2(s)$ by (22). If $\nabla_1(s)>0$ and $\nabla_2(s)>0$, calculate $\bar{K}(s)$ and $\bar{L}(s)$ by (21) to obtain $K(s)$ and $L(s)$, and then proceed to ***Step 4***; otherwise, go to ***Step 5***.

Step 3. Calculate $\Delta(s)$ by (14). If $\Delta(s)>0$, go to ***Step 4***; otherwise, go to ***Step 5***.

Step 4. Calculate $\mathcal{P}(s)$ and $\mathcal{Q}(s)$ by solving the coupled backward recursive RDEs in (13) and (20), respectively. If $s\neq 0$, set $s=s-1$ and return to ***Step 2***.

Step 5. If any of the conditions $\Delta(s)>0$, $\nabla_1(s)>0$,$\nabla_2(s)>0$, $\mathcal{P}(0)\leq\gamma^2\mathcal{W}$ are not satisfied, this algorithm is infeasible. Stop.

Remark 4. *This study has focused on MASs operating under the multi-Round-Robin scheduling rule, with the aim of investigating the finite-horizon H_∞ consensus control problem. First, a tractable multi-Round-Robin protocol scheduling model has been established, which effectively characterizes the scheduling behavior of network resources by introducing a binary matrix. Building on this foundation and incorporating information interaction mechanisms among agents, a H_∞ consensus control strategy has been further derived through the analysis of dynamic characteristics of consensus errors. In Theorem 1, sufficient conditions have been provided for the system to satisfy the H_∞ performance criterion. In Theorem 2, the consensus controller gain and observer gain that guarantee the H_∞ performance have been designed.*

Remark 5. *Compared with existing studies on consensus control of MASs under communication protocols, this paper makes two key contributions: (1) it is the first to investigate the finite-horizon H_∞ consensus control for time-varying MASs under the multi-Round-Robin protocol; and (2) a novel and tractable multi-Round-Robin model has been established, which not only offers operational flexibility and practicality, but also significantly reduces modeling complexity by employing a binary stochastic matrix to characterize the scheduling behavior.*

4. A Numerical Example

In this section, a numerical example is presented to validate the effectiveness of the proposed observer-based consensus control algorithm.

Consider a time-varying MAS comprising five agents, where the dynamic of each agent is described by (1). The communication topology is represented by a directed weighted graph $\mathcal{G}(\mathcal{V}, \mathcal{E}, \mathcal{H})$ with $\mathcal{V} = \{1, 2, 3, 4, 5\}$, as shown in Figure 2.

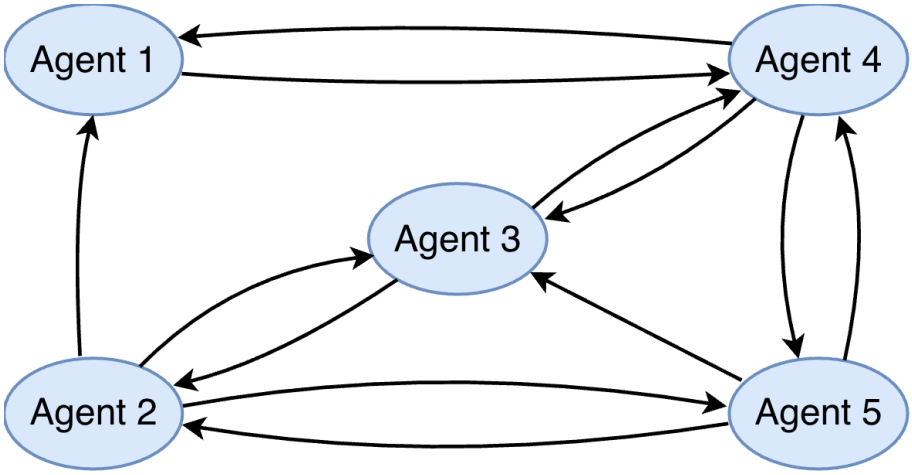

Figure 2. The communication topology for the time-varying MAS.

The corresponding adjacent matrix $\mathcal{H}$ is given by

$$\mathcal{H} = \begin{bmatrix} 0 & 1 & 0 & 1 & 0 \\ 0 & 0 & 1 & 0 & 1 \\ 0 & 1 & 0 & 1 & 1 \\ 1 & 0 & 1 & 0 & 1 \\ 0 & 1 & 0 & 1 & 0 \end{bmatrix}.$$

Under the multi-Round-Robin protocol, the number of neighbors selected for each agent at each time step is set as $\iota_1 = \iota_3 = \iota_5 = 1$ and $\iota_2 = \iota_4 = 2$.

The system parameters of each agent are given by

$$\begin{aligned} A(s) &= \begin{bmatrix} 0.98 + 0.01\cos(0.5s) & -0.5 \\ -0.1 & -0.5 - 0.1\sin(0.3s) \end{bmatrix}, \\ B(s) &= \begin{bmatrix} 0.2 - 0.05\sin(0.4s) \\ 0.24 \end{bmatrix}, \quad M(s) = \begin{bmatrix} 0.15 & 0 \\ 0 & 0.15 \end{bmatrix}, \\ C(s) &= [1.35 \quad 0.84],\ F(s) = -0.4,\ E(s) = [0.26 \quad 0.24]^T. \end{aligned}$$

The external disturbances $\omega_i(s)$ and $\nu_i(s)$ are chosen as follows:

$$\begin{aligned} &\omega_1(s) = 0.8\cos(1.2s), \qquad \omega_2(s) = 0.8\sin(0.7s), \\ &\omega_3(s) = 0.8\sin(1.3s), \qquad \omega_4(s) = 0.8\cos(0.6s), \\ &\omega_5(s) = 0.5\sin(0.45s) + 0.4\cos(0.7s), \\ &\nu_1(s) = 0.8\sin(1.2s), \qquad \nu_2(s) = 0.8\sin(0.7s), \\ &\nu_3(s) = 0.8\cos(s), \qquad \nu_4(s) = 0.8\cos(0.5s), \\ &\nu_5(s) = 0.4\sin(0.8s) + 0.4\cos(0.6s). \end{aligned}$$

The initial states $x_i(0)$ for $i \in \mathcal{V}$ are chosen as

$$\begin{aligned} &x_1(0) = [3.2 \quad 1.6]^T, \qquad x_2(0) = [4.8 \quad -0.4]^T, \\ &x_3(0) = [-1 \quad -3.6]^T, \qquad x_4(0) = [1.2 \quad -0.5]^T, \\ &x_5(0) = [2.5 \quad -3.5]^T. \end{aligned}$$

In this numerical example, the parameters for the H_∞ performance criterion and cost function are set as $\gamma = 0.95$, $W = 9.8I$, $\varepsilon_1 = 0.002$, and $\varepsilon_2 = 0.003$.

By conducting Algorithm 1, the observer gains and controller gains are obtained, under which, the simulation results over the time horizon $s \in [0, 80]$ are presented in Figures 3–6. As shown in Figure 3, the open-loop system exhibits unstable behavior, with the state trajectories of all five agents diverging over time, demonstrating the necessity of implementing a consensus control strategy. With the proposed observer-based control scheme, Figure 4 show that the state observer successfully tracks the actual states of all agents, providing accurate state estimation for the controller design despite the presence of external disturbances. For this open-loop unstable MAS, the simulation results reveal that the proposed consensus control strategy successfully drives the system to achieve consensus, and the observer-based controller effectively suppresses external disturbances for all agents.

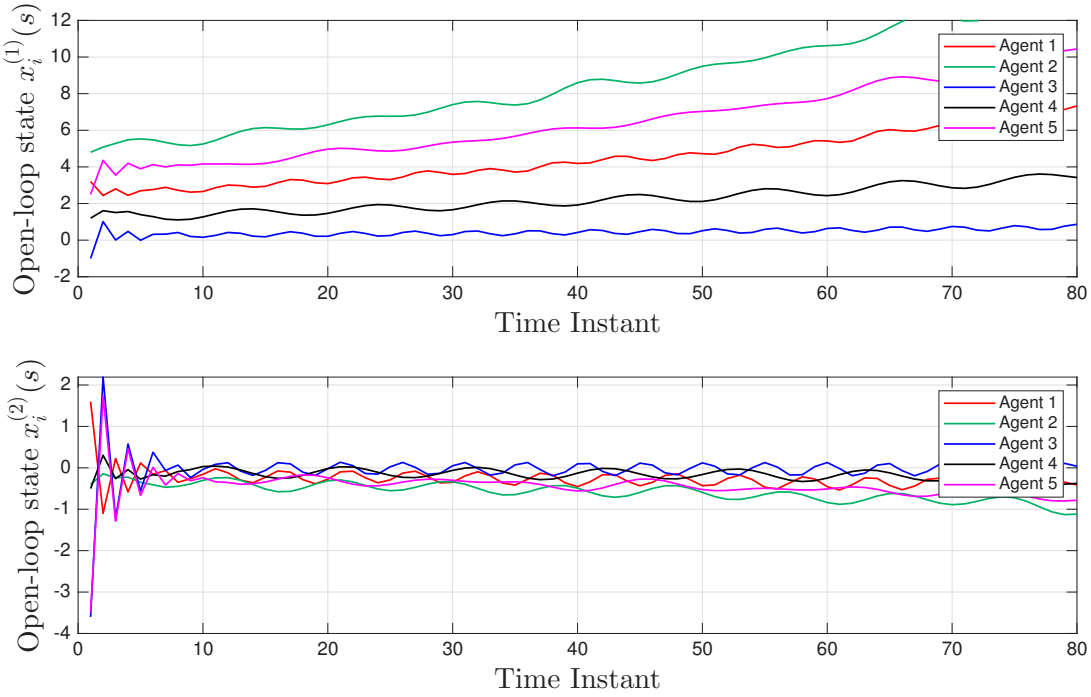

Figure 3. Open-loop state trajectories of all agents.

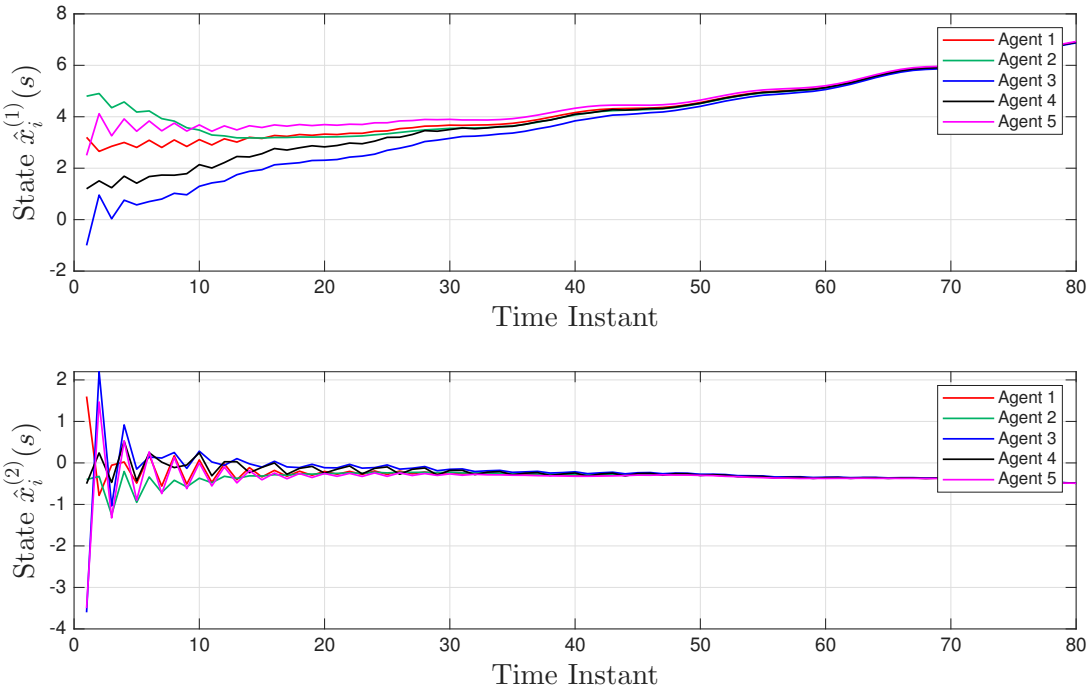

Figure 4. Estimated state trajectories of all agents.

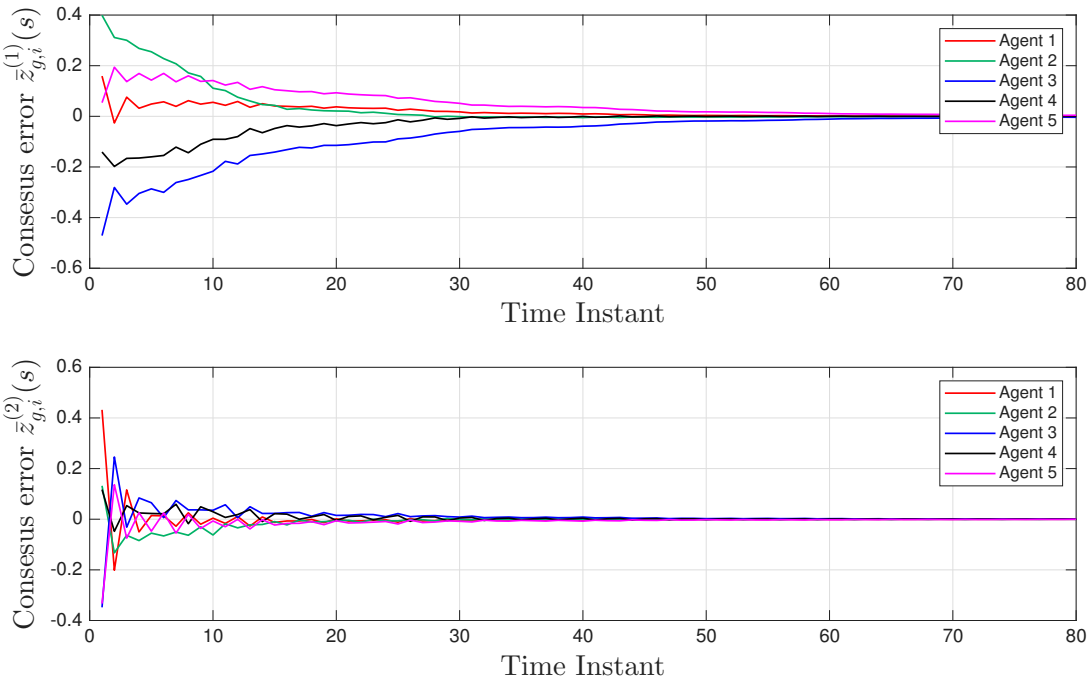

Figure 5. Consensus error trajectories of all agents.

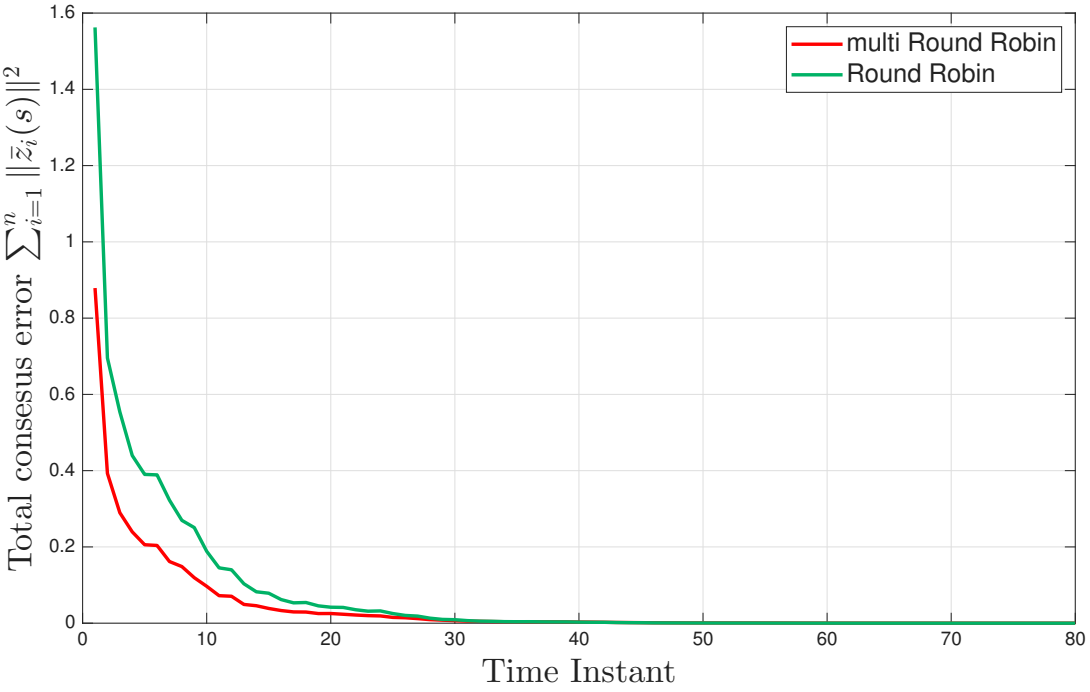

Figure 6. Comparison of total consensus error under the multi-Round-Robin and Round-Robin protocols.

The convergence behavior of system (1) is evaluated through consensus errors (Figure 5) show that the consensus errors converge asymptotically, indicating that all agents successfully reach a common consensus state. The comparative analysis of these error profiles validates that the proposed consensus control strategy effectively achieves the consensus objectives through local information exchange. Furthermore, the simulation results confirm that the multi-Round-Robin protocol scheduling mechanism successfully manages the network resource allocation, enabling efficient information exchange among neighboring agents while maintaining the desired H_∞ consensus performance. Figure 6 compares the total consensus error under the multi-Round-Robin and Round-Robin protocols, showing that the multi-Round-Robin protocol achieves a faster consensus convergence rate.

5. Conclusions

This paper has investigated the H_∞ consensus control problem for time-varying MASs under multi-Round-Robin scheduling. An integrated observer and finite-horizon consensus control strategy has

been adopted to achieve anti-disturbance and robust performance. By constructing appropriate Lyapunov functions and applying the completing squares method, sufficient conditions have been derived to guarantee the H_∞ performance of the time-varying MAS. Furthermore, an observer-based H_∞ weighted consensus controller has been designed over a directed weighted graph by solving two backward recursive RDEs. A numerical example has been provided to illustrate the effectiveness of the proposed algorithm. Future research will extend the core contributions of this work to MASs with relay-assisted communications, while also considering a broader set of performance objectives (see, e.g., [44–49]).

Author Contributions

J.C.: methodology, writing—original draft, software; Y.W.: methodology, writing—reviewing and editing, funding acquisition; F.W.: supervision, funding acquisition. All authors have read and agreed to the published version of the manuscript.

Funding

This work is supported by the National Natural Science Foundation of China (Grant No. 62503235), the Startup Foundation for Introducing Talent of NUIST (Grant No. 1083142501018), and the Fundamental Science (Natural Science) Research Project of Higher Education Institutions of Jiangsu Province (Grant No. 25KJB413007).

Institutional Review Board Statement

Not applicable. This study did not involve human participants or animals.

Informed Consent Statement

Not applicable.

Data Availability Statement

Not applicable.

Conflicts of Interest

The authors declare no conflict of interest.

Use of AI and AI-Assisted Technologies

No AI tools were utilized for this paper.

References

1. Feriani, A.; Hossain, E. Single and multi-agent deep reinforcement learning for AI-enabled wireless networks: A tutorial. *IEEE Commun. Surv. Tutor.* **2021**, *23*, 1226–1252.
2. Zhao, G.; Lin, K.; Chapman, D.; et al. Optimizing energy efficiency of LoRaWAN-based wireless underground sensor networks: A multi-agent reinforcement learning approach. *Internet Things* **2023**, *22*, 100776.
3. Ren, H.; Wang, Y.; Liu, M.; et al. An optimal estimation framework of multi-agent systems with random transport protocol. *IEEE Trans. Signal Process.* **2022**, *70*, 2548–2559.
4. Zhang, B.; Hu, W.; Ghias, A.M.; et al. Multi-agent deep reinforcement learning based distributed control architecture for interconnected multi-energy microgrid energy management and optimization. *Energy Convers. Manag.* **2023**, *277*, 116647.
5. Wang, Y.; Qiu, D.; Teng, F.; et al. Towards microgrid resilience enhancement via mobile power sources and repair crews: A multi-agent reinforcement learning approach. *IEEE Trans. Power Syst.* **2023**, *39*, 1329–1345.
6. Jia, M.; Cui, Z.; Hug, G. Enhancing LLMs for power system simulations: A feedback-driven multi-agent framework. *IEEE Trans. Smart Grid* **2025**, *16*, 5556–5572.
7. Hou, Y.; Zhao, J.; Zhang, R.; et al. UAV swarm cooperative target search: A multi-agent reinforcement learning approach. *IEEE Trans. Intell. Veh.* **2023**, *9*, 568–578.
8. Yan, Z.; Han, L.; Li, X.; et al. Event-triggered formation control for time-delayed discrete-time multi-agent system applied to multi-UAV formation flying. *J. Frankl. Inst.* **2023**, *360*, 3677–3699.
9. Peng, Z.; Wu, G.; Luo, B.; et al. Multi-UAV cooperative pursuit strategy with limited visual field in urban airspace: A multi-agent reinforcement learning approach. *IEEE/CAA J. Autom. Sin.* **2025**, *12*, 1350–1367.
10. Dong, J.; Yassine, A.; Armitage, A.; et al. Multi-agent reinforcement learning for intelligent V2G integration in future transportation systems. *IEEE Trans. Intell. Transp. Syst.* **2023**, *24*, 15974–15983.

11. Wang, T.; Cao, J.; Hussain, A. Adaptive traffic signal control for large-scale scenario with cooperative group-based multi-agent reinforcement learning. *Transp. Res. Part C Emerg. Technol.* **2021**, *125*, 103046.
12. Huang, S.; Sun, C.; Wang, R.-Q.; et al. Toward adaptive and coordinated transportation systems: A multi-personality multi-agent meta-reinforcement learning framework. *IEEE Trans. Intell. Transp. Syst.* **2025**, *26*, 12148–12161.
13. Wang, Q.; Dong, X.; Wang, B.; et al. Finite-time observer-based H_∞ fault-tolerant output formation tracking control for heterogeneous nonlinear multi-agent systems. *IEEE Trans. Netw. Sci. Eng.* **2023**, *10*, 1822–1834.
14. Zou, L.; Wang, Z.; Gao, H.; et al. Finite-horizon H_∞ consensus control of time-varying multi-agent systems with stochastic communication protocol. *IEEE Trans. Cybern.* **2017**, *47*, 1830–1840.
15. Zhang, J.; Zhang, H.; Wang, W.; et al. Adaptive dynamic event-triggered distributed output observer for leader-follower multi-agent systems under directed graphs. *IEEE Trans. Neural Netw. Learn. Syst.* **2023**, *35*, 17440–17449.
16. Zhong, Y.; Lyu, G.; He, X.; et al. Distributed active fault-tolerant cooperative control for multi-agent systems with communication delays and external disturbances. *IEEE Trans. Cybern.* **2021**, *53*, 4642–4652.
17. Chen, J.; Chen, B.; Zeng, Z. Adaptive dynamic event-triggered fault-tolerant consensus for nonlinear multi-agent systems with directed/undirected networks. *IEEE Trans. Cybern.* **2023**, *53*, 3901–3912.
18. Wei, B.; Tian, E.; Gu, Z.; et al. Quasi-consensus control for stochastic multi-agent systems: When energy harvesting constraints meet multimodal FDI attacks. *IEEE Trans. Cybern.* **2024**, *54*, 1755–1767.
19. Liu, D.; Jiang, K.; Xiong, P.; et al. Fixed-time quasi-consensus energy management method for battery energy storage systems in DC microgrids under two types of DoS attacks. *J. Energy Storage* **2025**, *113*, 115574.
20. Yu, L.; Wang, Z.; Liu, Y.; et al. Sampled-data nonfragile bipartite tracking consensus for nonlinear multi-agent systems: Dealing with denial-of-service attacks. *IEEE Trans. Syst. Man Cybern. Syst.* **2024**, *55*, 1202–1214.
21. Zhou, Q.; Yin, C.; Ma, H.; et al. Prescribed performance bipartite consensus control for MASs under data-driven strategy. *IEEE/CAA J. Autom. Sin.* **2025**, *12*, 937–946.
22. Zhang, Z.; Chen, S.; Zheng, Y. Fully distributed scaled consensus tracking of high-order multi-agent systems with time delays and disturbances. *IEEE Trans. Ind. Inform.* **2022**, *18*, 305–314.
23. Shang, Y. Scaled consensus and reference tracking in multiagent networks with constraints. *IEEE Trans. Netw. Sci. Eng.* **2022**, *9*, 1620–1629.
24. Olfati-Saber, R.; Fax, J.A.; Murray, R.M. Consensus and cooperation in networked multi-agent systems. *Proc. IEEE* **2007**, *95*, 215–233.
25. Schiz, T.; Ebel, H. Reducing the communication of distributed model predictive control: Autoencoders and formation control. *Control Eng. Pract.* **2025**, *165*, 106560.
26. Bai, J.; Yuan, S.; Zhang, D.; et al. Output feedback sliding mode control for two-time-scale fuzzy systems with stochastic communication protocol. *Commun. Nonlinear Sci. Numer. Simul.* **2026**, *153*, 109524.
27. Li, C.; Liu, Y.; Gao, M.; et al. Fault-tolerant formation consensus control for time-varying multi-agent systems with stochastic communication protocol. *Int. J. Netw. Dyn. Intell.* **2024**, *3*, 100004.
28. Geng, H.; Wang, Z.; Chen, Y.; et al. Variance-constrained filtering fusion for nonlinear cyber-physical systems with the denial-of-service attacks and stochastic communication protocol. *IEEE/CAA J. Autom. Sin.* **2022**, *9*, 978–989.
29. Chen, W.; Ding, D.; Dong, H.; et al. Finite-horizon H_∞ bipartite consensus control of cooperation-competition multi-agent systems with Round-Robin protocols. *IEEE Trans. Cybern.* **2021**, *51*, 3699–3709.
30. Li, B.; Wang, Z.; Han, Q.-L.; et al. Distributed quasiconsensus control for stochastic multi-agent systems under Round-Robin protocol and uniform quantization. *IEEE Trans. Cybern.* **2022**, *52*, 6721–6732.
31. Wu, Y.; Niu, Y.; Yang, Y. Security sliding mode control for T-S fuzzy systems under attack probability-dependent dynamic round-robin protocol. *Int. J. Syst. Sci.* **2024**, *55*, 926–940.
32. Liu, J.; Gong, E.; Zha, L.; et al. Observer-based security fuzzy control for nonlinear networked systems under weighted try-once-discard protocol. *IEEE Trans. Fuzzy Syst.* **2023**, *31*, 3853–3865.
33. Wang, J.; Yang, C.; Xia, J.; et al. Observer-based sliding mode control for networked fuzzy singularly perturbed systems under weighted try-once-discard protocol. *IEEE Trans. Fuzzy Syst.* **2022**, *30*, 1889–1899.
34. Xu, J.; Niu, Y.; Lv, X.; et al. Sliding mode consensus control for multi-agent systems under component-based weighted try-once-discard protocol. *Int. J. Syst. Sci.* **2023**, *54*, 2566–2578.
35. Fan, S.; Meng, M.; Fu, Y.; et al. Distributed adaptive tracking control for fuzzy nonlinear MASs under Round-Robin protocol. *IEEE Trans. Fuzzy Syst.* **2025**, *33*, 1488–1498.
36. Bu, X.; Jin, S.; Bu, X.; et al. Fully distributed data-driven consensus tracking for multiple high-speed trains with sensor resolution under Round-Robin protocol. *IEEE Internet Things J.* **2026**, *3*, 100004.
37. Liu, J.; Zheng, H.; Zha, L.; et al. Secure consensus for multi-agent systems with hybrid cyber attacks: A multi-Round-Robin protocol-based approach. *Inf. Sci.* **2024**, *677*, 120878.
38. Zeng, P.; Deng, F.; Zhang, H.; et al. Event-based H_∞ control for discrete-time fuzzy Markov jump systems subject to DoS attacks. *IEEE Trans. Fuzzy Syst.* **2022**, *30*, 1853–1863.
39. Zhang, H.; Yan, H.; Qiu, J. Finite-horizon H_∞ consensus control of discrete time-varying multiagent systems: A dynamic event-based learning approach. *IEEE Trans. Autom. Control* **2023**, *68*, 6270–6276.

40. Zhang, Y.; Xiang, Z. Prescribed-Time Optimal Control for a Class of Switched Nonlinear Systems. *IEEE Trans. Autom. Sci. Eng.* **2025**, *22*, 3033–3043.
41. Donkers, M.C.F.; Heemels, W.P.M.H.; van de Wouw, N.; et al. Stability Analysis of Networked Control Systems Using a Switched Linear Systems Approach. *IEEE Trans. Autom. Control* **2011**, *56*, 2101–2115.
42. Liu, K.; Selivanov, A.; Fridman, E. Survey on time-delay approach to networked control. *Annu. Rev. Control* **2019**, *48*, 57–79.
43. Horn, R.A.; Johnson, C.R. *Topics in Matrix Analysis*; Cambridge University Press: Cambridge, UK, 1994.
44. Jia, C.; Hu, J.; Yi, X.; et al. Recursive state estimation for a class of quantized coupled complex networks subject to missing measurements and amplify-and-forward relay. *Inf. Sci.* **2023**, *630*, 53–73.
45. Wang, F.; Wang, Z.; Liang, J.; et al. Recursive filtering for two-dimensional systems with amplify-and-forward relays: Handling degraded measurements and dynamic biases. *Inf. Fusion* **2024**, *108*, 102368.
46. Tan, H.; Shen, B.; Li, Q.; et al. Recursive filtering for stochastic systems with filter-and-forward successive relays. *IEEE/CAA J. Autom. Sin.* **2024**, *11*, 1202–1212.
47. Zhang, W.; Wang, N.; Song, Y.; et al. Dynamic output-feedback model predictive control for polytopic uncertain systems with amplify-and-forward relays. *J. Frankl. Inst.* **2023**, *360*, 11055–11074.
48. Hu, J.; Li, J.; Yan, H.; et al. Optimized distributed filtering for saturated systems with amplify-and-forward relays over sensor networks: A dynamic event-triggered approach. *IEEE Trans. Neural Netw. Learn. Syst.* **2024**, *35*, 17742–17753.
49. Hou, Q.; Dong, J. Distributed event-triggered consensus control for multi-agent systems with guaranteed performance and positive inter-event times. *IEEE Trans. Autom. Sci. Eng.* **2024**, *21*, 746–757.